An Advanced Compressor for Turbo-Brayton Cryocoolers

R.W. Hill, J.K. Hilderbrand, M.V. Zagarola

Creare Inc.
Hanover, NH 03755

ABSTRACT

Future space-borne infrared sensor missions will require reliable, efficient, and lightweight cryocoolers. Reverse turbo-Brayton cryocoolers have the inherent benefits of negligible vibration emittance and the ability to cool remote or distributed loads. In this paper we describe the results of our efforts to improve overall system efficiency with the development of a high performance permanent magnet motor compressor. A prototype 500 W class compressor was fabricated and tested at prototypical operating conditions. The compressor utilizes gas bearings for zero-wear, negligible vibration, and high-speed operation; and a miniature impeller for high performance at relatively low power levels. The impeller was manufactured using new fabrication processes that allow advanced blade geometries to be produced at a miniature scale. In addition, the new process is extremely precise, simplifies inspection, is readily scalable to different power levels, and produces parts more quickly and at a lower cost than the heritage process. The compressor tests demonstrated a reduction in input power of up to 30% as compared to our induction-motor compressors. We expect further performance improvements as we add upgrades to the prototype.

INTRODUCTION

Future space missions for the Department of Defense (DoD) and NASA may require mechanical cryocoolers for cooling infrared detectors. These cryocoolers will need to be efficient, lightweight, and highly reliable to meet mission objectives. Typical cooling loads range from hundreds of milliwatts at 10 K to several watts at 35 K up to approximately 10 W at 70 K, depending on the specific focal plane technology and size, with additional loads at higher temperatures for cooling optics and for shielding. The dual cooling loads are usually absorbed using a two-stage cryocooler, which has benefits in terms of size and mass relative to two single-stage coolers. In addition, low exported vibration is a key requirement for missions where precise pointing accuracy is required. Low vibration is difficult to achieve with Stirling-class cryocooler technologies which utilize reciprocating compressors (and expanders in some cases). Vibration cancellation techniques have been demonstrated to reduce exported vibration to below 100 mN,[1] but this value is still unacceptable for some missions. Turbo-Brayton cryocoolers offer a very low vibration alternative. These cryocoolers utilize gas-bearing turbomachines with miniature precisely balanced rotors to compress and expand the working gas. The result is almost imperceptible exported vibration without the need for vibration cancellation.

A single turbo-Brayton cooler has been space flight qualified and implemented in a space application. The NICMOS Cryogenic Cooler (NCC) is a single-stage turbo-Brayton cryocooler

Cryocoolers 16, edited by S.D. Miller and R.G. Ross, Jr.

that was installed on the Hubble Space Telescope (HST) in early 2002.[2] This cryocooler provides 7 W of cooling at 70 K to the NICMOS instrument, replacing the solid nitrogen cryogen that had prematurely depleted. The NCC returned the instrument to operation within one month of installation and maintained the instrument at the optimum temperature for over six years. Other programs have successfully demonstrated the technology at temperatures of 35 K[3] and at even lower temperatures.[4] Advanced development programs are focused on components that are lighter, smaller and have higher performance. A recent program developed and demonstrated the next-generation recuperator.[5] This paper reviews our progress on developing a next-generation compressor for turbo-Brayton cryocoolers.

COMPRESSORS FOR TURBO-BRAYTON CRYOCOOLERS

The compressor is one of the major components of a turbo-Brayton cryocooler in addition to the turbine, recuperative heat exchanger, and electronics. Overall cryocooler efficiency and weight as well as the weight of the payload heat rejection system are strongly affected by the compressor performance. The compressor performance is best characterized by the powertrain efficiency, which is the ideal compressor work divided by the DC input power to the drive inverter (equation 1). This performance parameter accounts for losses in the compressor electronics, motor, bearings, and impeller. The power train efficiency can therefore be represented by the product of the inverter efficiency, motor efficiency, shaft efficiency, and the aerodynamic efficiency and is given by:

$$\eta_{pt} = \frac{\dot{m}\Delta h_s}{P_{dc}} = \eta_{Inv}\eta_{Motor}\eta_{Shaft}\eta_{Aero} \tag{1}$$

The powertrain efficiency of the NCC induction motor compressor is approximately 35 to 40%.

Figure 1 shows our projections for an advanced 400-500 W permanent magnet motor (PMM) compressor in comparison to our existing induction motor compressor technology. This figure compares the power train efficiency and each of the four contributing efficiencies. We estimated an improvement of aerodynamic efficiency could be achieved from about 65 to 70% with the NCC compressor to about 75% through modifications to the impeller and diffuser designs. Further improvements of the aerodynamics through design iterations and testing might improve the efficiency

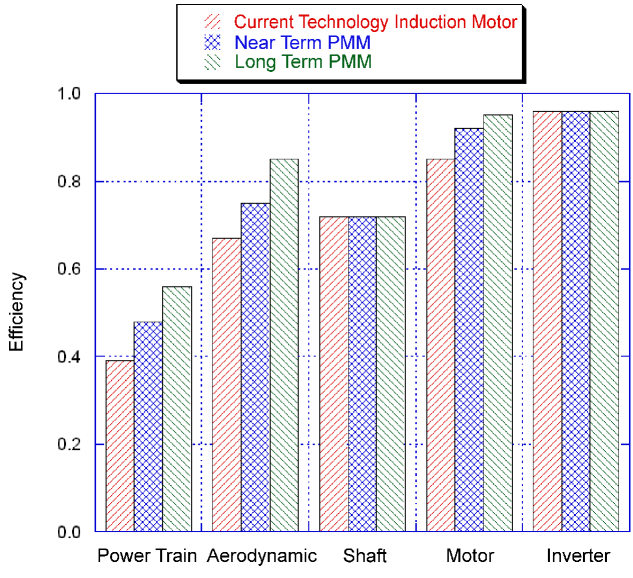

Figure 1. Efficiencies of existing induction motor compressor compared to projected performance of a high-efficiency PMM compressor.

to levels approaching 85% consistent with performance observed on larger turbomachines reported in open literature.[6]

In addition, we estimate that motor efficiencies on the order of 92 to 93% are possible based on our testing with 100 W capacity PMM compressors to higher capacity using the same materials. The induction motor efficiency is on the order of 85%. The efficiency improvement for the PMM motor is achieved by the elimination of the slip loss and a significant reduction in the magnetizing current in comparison to the induction motor. The efficiency of our laboratory inverters (on the order of 93 to 95%) is likely the best that can be achieved. Our expectation is that any further improvements in inverters would be to reduce their mass and achieve similar efficiencies. We expected that improvements to shaft efficiency could not be achieved without a significant departure from our heritage rotor diameters and gas bearing design.

Compressor Design

The advanced compressor design is shown in Figure 2. The design is based on the space qualified NCC compressor but is driven by a PMM which has been adapted from a previously tested 100 W design. The compressor utilizes a multipart rotor. A permanent magnet is fastened using epoxy within a hollow shaft to form the electromagnetic rotor. An advanced impeller is mechanically fastened to the shaft. Self-acting gas bearings provide radial and axial positioning of the rotor. These bearings are supported in a sleeve assembly that also contains the motor stator windings. The sleeve is designed to conduct any heat dissipated in the windings and generated by the bearings to a copper bearing housing that is part of the compressor thermal management system. Heat is conducted in this housing to the base plate where it is removed by the spacecraft thermal management system. The journal bearing diameter is 6.4 mm (0.25 in.) and the impeller diameter is 19 mm (0.75 in.). The 19 mm (0.75 in.) diameter represents a departure in heritage from our 15 mm (0.6 in.) design for the 300-400 W class induction motor compressor and is based on a trade study to minimize journal bearing and disk friction losses.

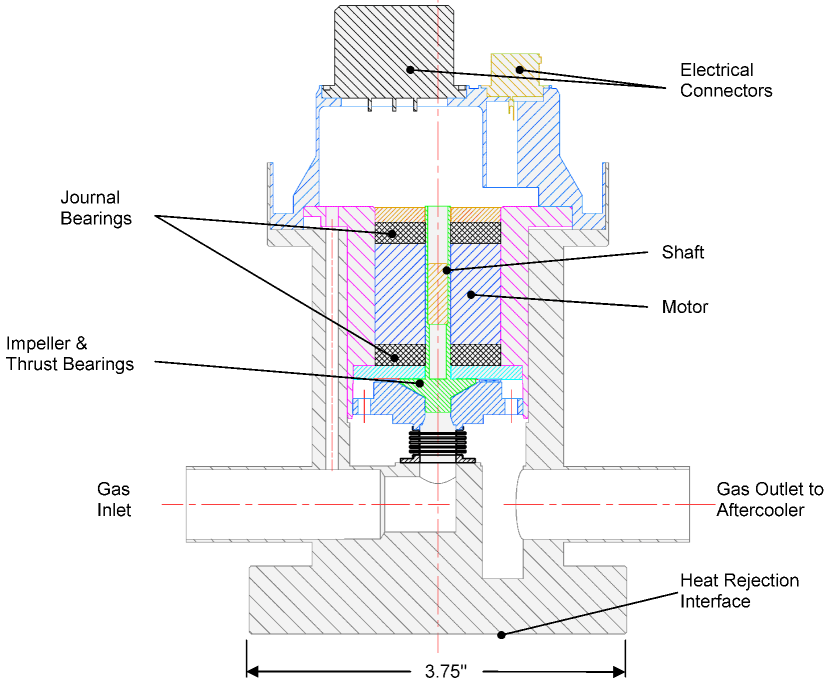

Figure 2. 400-500 W class PMM compressor design.

We developed a detailed compressor computational fluid dynamics (CFD) model to evaluate the internal temperatures during normal operation. Based on the estimated temperatures in the magnet region, we chose to use a Samarium Cobalt (SmCo) magnet instead of the heritage Neodymium-Iron-Boron (NdFeB) magnet since the SmCo is capable of higher temperature operation before a risk of demagnetization occurs. The SmCo has the disadvantage of slightly higher motor losses.

We developed an advanced impeller blade design to improve the aerodynamic efficiency of the rotor. Analyses were performed to predict the performance of our heritage 15 mm (0.6 in.) impeller design for which we had head-flow performance test data. The blade design for a new 19 mm (0.75 in.) impeller was then developed having a predicted improvement in aerodynamic efficiency and head-flow performance.

We performed tests to demonstrate a new fabrication approach for our impellers using a CNC process to cut the blades followed by a diffusion bonding process and final machining instead of our heritage approach of using an EDM process to cut the flow passages. We performed diffusion bonding trials to establish a combination of furnace temperature, compression load, and time at temperature to achieve acceptable bonded performance. Bonding trials were performed using the heritage blade geometry based on our 15 mm (0.6 in.) impellers, as well as with the 19 mm (0.75 in.) impeller with the advanced blade design. The advanced geometry impellers prior to diffusion bonding are shown in Figure 3. Figure 4 provides a photograph of the final machined advanced geometry impeller and the compressor rotor after the impeller has been attached to the shaft.

COMPRESSOR PERFORMANCE

To conduct the performance testing, the compressor was installed in an existing compressor test loop (Figure 5). The test loop consists of all the equipment—the plumbing, valves, instrumentation, coolant loop, and compressor inverter—required to execute a compressor performance test. We performed five runs to gather compressor performance data. The first three runs were all per-

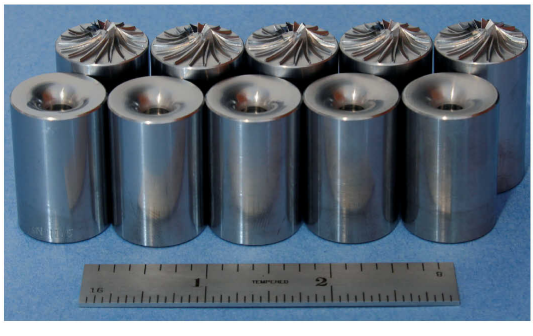

Figure 3. Advanced geometry compressor impeller components after machining prior to diffusion bonding.

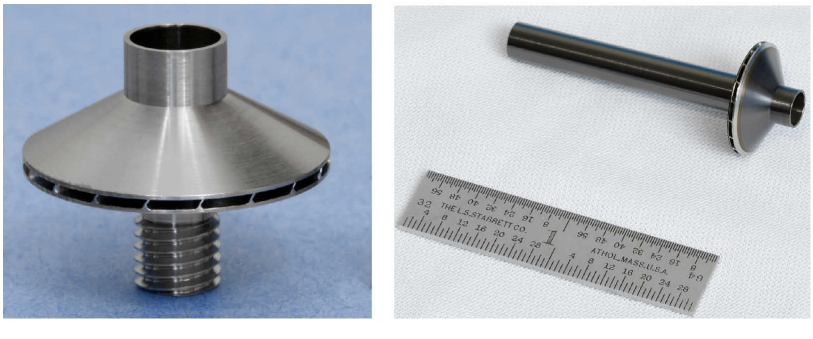

Figure 4. Finish machined advanced geometry impeller (left) and final rotor assembly (right).

formed with a neon system fill that provided a static loop pressure of 1.4 bar (5 psig), and we obtained data at shaft speeds of 4500, 5000, and 5500 rev/s. We then decreased the system pressure and performed runs of 4500 and 5000 rev/s.

Figure 6 shows the power train efficiency observed in the PMM compressor testing. Around a typical flow coefficient operating point of 0.20 to 0.22, the measured efficiency is around 46%. This power train efficiency represents a considerable improvement over the power train efficiency

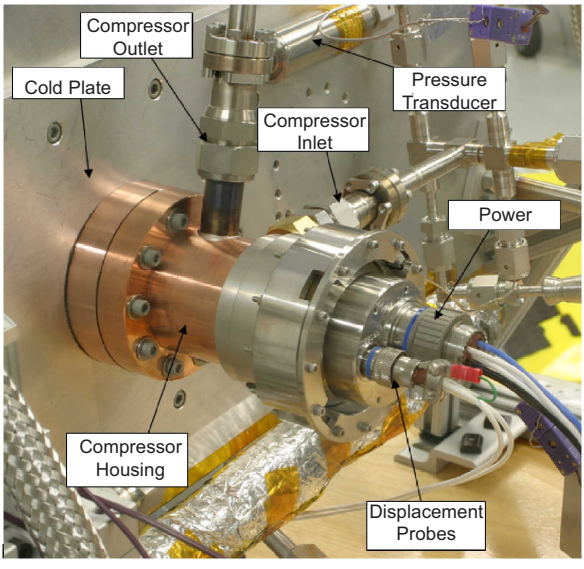

Figure 5. Advanced PMM compressor installed in the test facility.

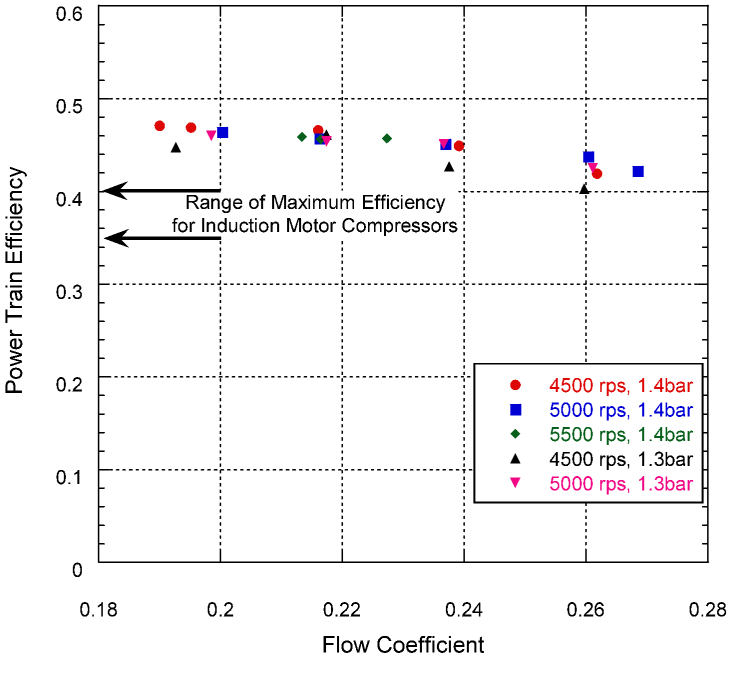

Figure 6. Measured power train efficiency.

for induction motor compressors of similar size (less than 40%), and corresponds to a reduction in input power of up to 30% as compared to our induction-motor compressors. Testing of this compressor was limited to pressures and Reynolds numbers below prototypical values. We expect further improvements in compressor performance as we continue with our development and refinement of this PMM prototype compressor.

CONCLUSIONS AND RECOMMENDATIONS

The design of a 400 to 500 W class PMM compressor for reverse Brayton cryocooler applications is complete. A new impeller fabrication process has been successfully demonstrated. The process is more precise, easier to inspect, and produces parts more quickly than the heritage EDM process. A prototype of the PMM compressor has been fabricated and tested at prototypical rotational speeds. The demonstrated compressor power train efficiency significantly exceeds that for our induction motor compressor and will result in a reduction of compressor input power of up to 30%. Our testing was limited to machine Reynolds numbers that are a factor of two to four below expected prototypical design operating conditions for the PMM compressor. Due to the sensitivity of compressor performance with Reynolds number, we expect that a higher performance can be demonstrated with a full power test of the PMM compressor.

ACKNOWLEDGMENT

The support and guidance of the Missile Defense Agency, the Air Force Research Laboratory, and NASA are gratefully acknowledged.

REFERENCES

1. Kirkconnell, C.S., Zagarola, M.V., and Russo, J.T., “Hybrid Stirling / Reverse Brayton and Multi-Stage Brayton Cryocoolers for Space Applications,” *Adv. in Cryogenic Engineering*, Vol. 51, Amer. Institute of Physics, Melville, NY (2006), pp. 1489-1496 .
2. Swift, W. L., Dolan, F. X., and Zagarola, M. V., “The NICMOS Cooling System – 5 Years of Successful OnOrbit Operation,” *Adv. in Cryogenic Engineering*, Vol. 53, Amer. Institute of Physics, Melville, NY (2008), pp. 799-806.
3. Zagarola, M. V., Dietz, A. J., Swift, W., and Davis, T., “35 K Turbo-Brayton Cryocooler Technology,” *Adv. in Cryogenic Engineering*, Vol. 49, Amer. Institute of Physics, Melville, NY (2004), pp. 1635-1642.
4. Swift, W. L., Zagarola, M. V., Breedlove, J. J., McCormick, J. A., and Sixsmith, H., “Initial Test Results From a 6–10 K Turbo-Brayton Cryocooler for Space Applications,” *Adv. in Cryogenic Engineering*, Vol. 49, Amer. Institute of Physics, Melville, NY (2004), pp. 1643-1649.
5. Hill, R.W., Izenson, M.G., Chen, W.B., and Zagarola, M.V., “A Recuperative Heat Exchanger for Space-Borne Turbo-Brayton Cryocoolers,” *Cryocoolers 14*, ICC Press, Boulder, CO (2007), pp. 525-533.
6. Balje, O. E., *Turbomachines: A Guide to Design, Selection, and Theory*, John Wiley & Sons, Inc., New York (1981).